Electronic Supporting Information

Facile Access to Versatile Fluorescent Carbon Dots toward Light-Emitting Diodes

Xin Guo, Cai-Feng Wang, Zi-Yi Yu, Li Chen and Su Chen*
State Key Laboratory of Materials-Oriented Chemical Engineering and College of Chemistry and Chemical Engineering, Nanjing University of Technology, Nanjing 210009 (P. R. China)
Fax: (+86) 25-83172258 E-mail: chensu@njut.edu.cn

1. Experimental

Materials: Reagent-grade styrene (St) and glycidyl methacrylate (GMA) were purchased from Aldrich and used as received. Potassium persulfate (KPS) was ordered from Aladdin-reagent Ltd. (ShangHai, China) and purified by recrystallization from water before use. Reagent-grade *N, N*-dimethylformamide, ethanol, and *N*-Methyl pyrrolidone were supplied by Sinopharm Chemical Reagent Co., Ltd. (Shanghai, China) and used as purchased without further purification. High-purity water with the resistivity of greater than 18 M·cm^{-1} was used in the experiments.

Synthesis of PS-co-PGMA photonic crystals: A typical synthesis of monodispersed microspheres is as follows: 7.5 g of St was dissolved in 150 g of purified water in a 250 mL round flask, and the stirring speed was set at 250 rpm. After the solution was heated at 98 ^{o}C for 15 min, the polymerization was initiated by 15 g aqueous solution containing 0.0375 g KPS. As the reaction for the PS seed was kept for 1.5 h under constant stirring, a solution containing 0.5 g St, 1 g GMA and 0.0075 g KPS was added, and polymerization was allowed to continue for another 2 h at 98 ^{o}C. After the mixture was quenched with air, the end product was obtained.

Synthesis of CDs: The parent PS-*co*-PGMA photonic crystals were firstly evaporated at 70 ^{o}C. The resulting solid microspheres were ground into powder, placed in a quartz reaction boat and then transferred into a high-temperature tube furnace. Typically, the samples were pyrolyzed in the furnace at 200, 300 and 400 ^{o}C respectively for 2 h at a heating rate of 5 ^{o}C·min^{-1} under an inert N_2 atmosphere. After the sample was cooled to room temperature, the solid composite was mechanically ground in an agate mortar and pestle. The solution samples for characterization were

prepared by dispersing the carbon dots in purified water followed by centrifugation at 10000 rpm. The solid samples for characterization were prepared by directly pressing the ultrafine products into the condensed films.

Preparation of LEDs：The ultraviolet InGaN LED chips with the peak wavelength centered on 370 nm were used and attached on the bottom of the LED bases. The two threads on LED were prepared to connect to the power supply. Afterwards, the silicone was mixed with the CDs phosphor and put in a vacuum chamber to remove the bubbles. About 30 μL of the phosphor mixture was dispensed into the conventional cup-shaped void on the LED chip and thermally cured at 150 ^{o}C for 1h. Finally, the optical lenses were placed on the bottom of the LED chip and the voids were filled with the silicone. The ultima LEDs were then further cured at 150 ^{o}C for 1h. All the optical performances were carried out using ZWL-600 instrument with integral sphere.

Characterization

Transmission electron microscopy (TEM): The particle diameter and lattice fringes were examined with a JEOL JEM-2100 transmission electron microscope. A drop of corresponding carbon dot aqueous solution was placed on a copper grid that was left to dry before transferring into the TEM sample chamber. The particle diameter was estimated by using ImageJ software analysis of the TEM micrographs.

Spectroscopy: Fourier-transform infrared (FT-IR) spectra were recorded on a Nicolet 6700 FT-IR spectrometer. Raman study was performed using a Horiba HR 800 Raman system equipped with a 514.5 nm laser. UV-vis absorption spectra were recorded by a UV-vis spectrometer (Lambda 950, Perkin-Elmer). Photoluminescence measurements were carried out on a Varian Cary Eclipse spectrophotometer. EPR spectra were recorded in solid states at room temperature on an EMX-10/12 spectrometer (microwave frequency: 9.751 GHz; modulation amplitude: 3.0 G; microwave power: 19.920 mW). Time-correlated single-photon counting (TCSPC) data were performed on SLM 48000 spectrofluorometer using a 380 nm laser as the excitation source.

Quantum yield calculation: Quantum yield (QY) was measured according to established procedure (Lakowicz, J. R. Principles of Fluorescence Spectroscopy, 2nd Ed., 1999, Kluwer Academic/Plenum Publishers, New York) by using quinine sulfate in 0.10 M H_2SO_4 solution as the standard (Φ=0.54). The quantum yield was calculated using the following equation:

$$Q = Q_R \frac{I}{I_R} \frac{A_R}{A} \frac{n^2}{n^2{}_R}$$

Where Q is the quantum yield, I is the measured integrated emission intensity, A is the optical density and n is the refractive index (taken here as the refractive index of

the respective solvents). The subscript R refers to the reference fluorophore of known quantum yield.

The UV-Vis absorption spectrometer (Lambda 950, Perkin-Elmer) was used to determine the absorbance of the samples at 300 nm. The concentration of the samples for QY estimation should allow the first excitonic absorption peak to be below 0.05 in order to avoid any significant reabsorption. A Varian Cary Eclipse spectrophotometer with an excitation slit width of 0.25 and an emission slit width of 0.25 was used to excite the samples at 300 nm and to record their photoluminescence spectra.

2. Results

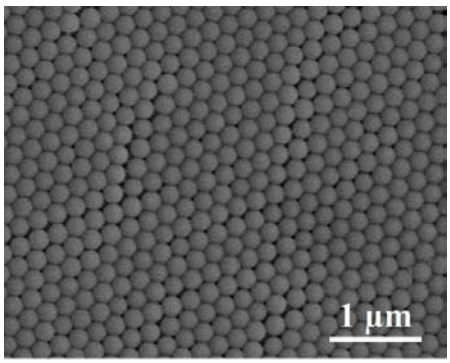

Figure S1. Typical SEM image of PS-*co*-PGMA photonic crystals.

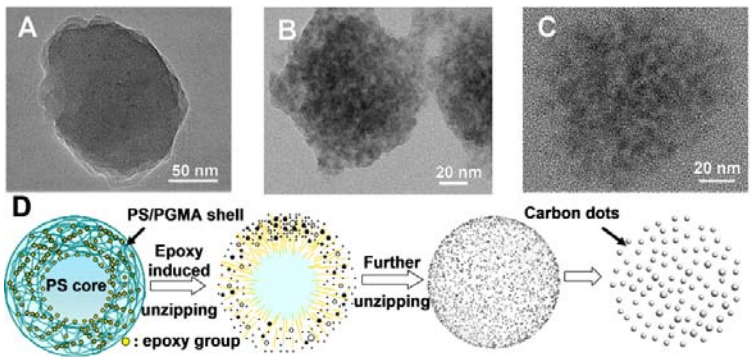

Figure S2. (A-C) Representative TEM images to elucidate the cracking evolution. (D) Schematic illustration for the generation of carbon dots derived from core-shell PS-*co*-PGMA microspheres.

The evolution process of the PS-*co*-PGMA microspheres cracked into CDs was deduced by TEM measurements, as seen in Figure S2A-C. We speculate that the microsphere undergo an unzipping mechanism during the pyrolysis process (Figure S2D), similar to the cases reported previously.[1] The epoxy group tethered to the surface of microspheres would energetically convert into more stable carbonyl pairs at

the preliminary stage of the pyrolysis procedure. The subsequent linear defects arise from the composition of fewer epoxy groups and more carbonyl groups make the microspheres fragile and easily fractured. Furthermore, the cracked ultrafine pieces surrounded by the mixed epoxy chains may further break up during the pyrolysis process, by which the bridging O atoms in the epoxy chains are transferred. Eventually, the CDs with various diameters were obtained.

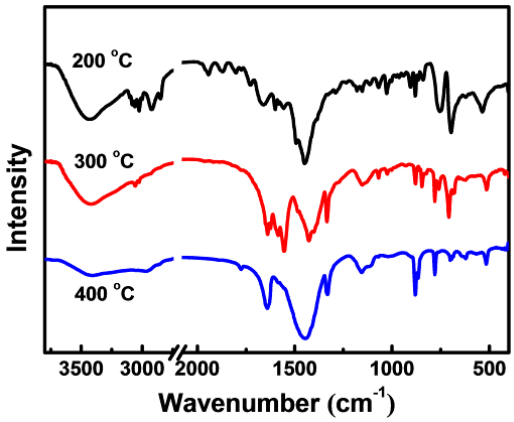

Figure S3. FT-IR spectra of the CDs obtained at different pyrolysis temperature.

Figure S3 show Fourier transform infrared (FT-IR) spectra of the CDs. The characteristic peaks near 3000 cm^{-1}, 1450 cm^{-1} correspond to the C=C stretch of polycyclic aromatic hydrocarbon, while the peaks at 1640 cm^{-1} and 1780 cm^{-1} are assigned to C=O stretching vibration. The peak near 3400 cm^{-1} is due to the -OH stretching mode.

Interestingly, the FT-IR spectra of CDs show a gradually disappear of the vibration band of epoxy groups at near 1060 cm^{-1} and an improving carbonyl signal at 1640 cm^{-1} and 1780 cm^{-1} as the pyrolysis temperature increased, which indicate that the epoxy group has been progressively converted.

Also, the decrease of signal at 700 cm^{-1} and 3400 cm^{-1}, along with the strengthen of 880 cm^{-1}, indicate the loss of hydrogen and the increase of π-conjugate system at higher temperature, meaning that diversiform polycyclic aromatic hydrocarbons could be generated under disparate unzipping degree at different temperature.

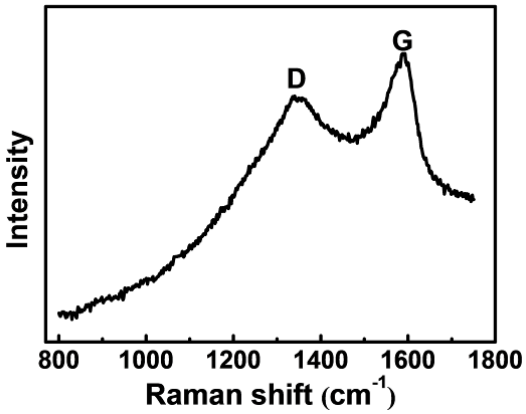

Figure S4. Raman spectrum of CD_{400}.

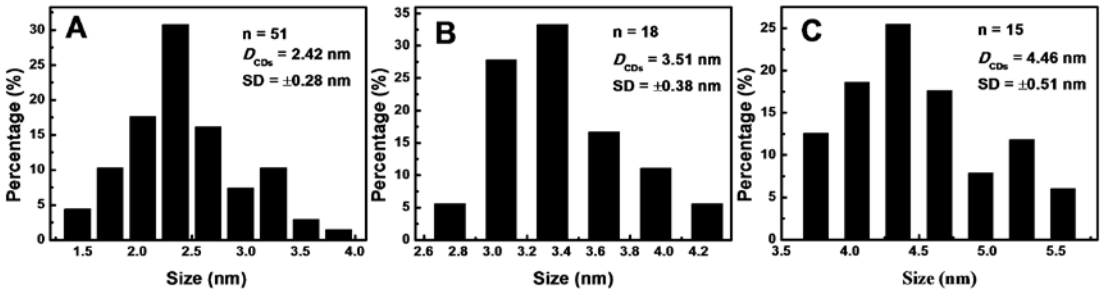

Figure S5. Size histograms of (A) CD_{200}, (B) CD_{300} and (C) CD_{400}, respectively. The data were derived from TEM images shown in Figure 2 by self-developed digital statistic software. The information of the number of particles counted (n), the mean particle diameter (D_{CDs}), and the standard deviation (SD) are also presented.

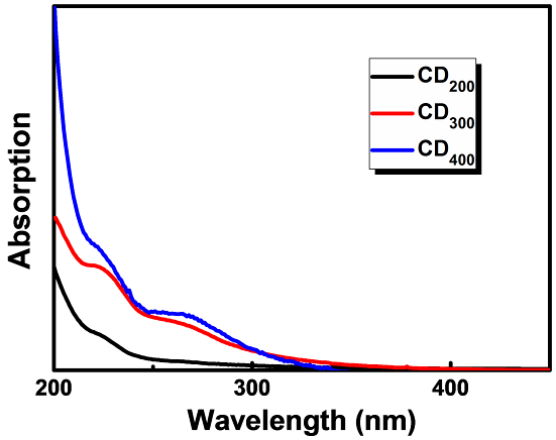

Figure S6. UV-vis spectra of CD_{200}, CD_{300} and CD_{400} in aqueous solution, respectively.

The UV-vis absorption spectra show typical absorption peaks between 220-300 nm, similar to those of reported CDs. [2]

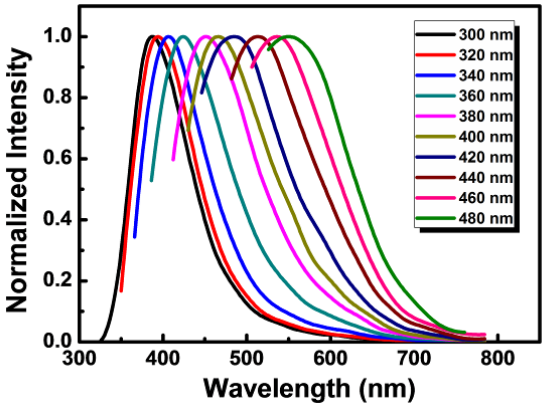

Figure S7. Normalized PL spectra of CD_{300} aqueous solution at different excitation wavelength (in 20 nm increment starting from 300 nm to 480 nm).

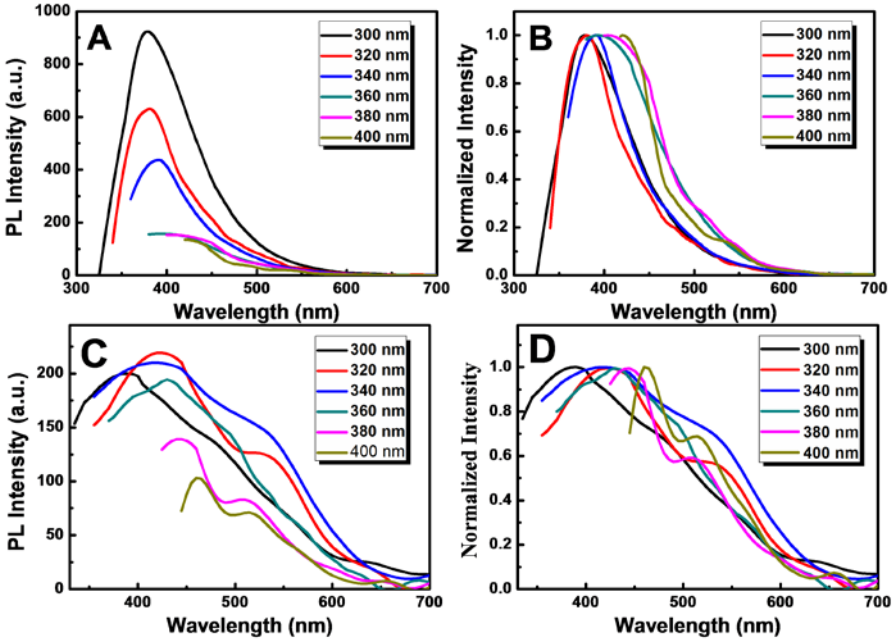

Figure S8. PL spectra and normalized spectra of (A, B) CD_{200} and (C, D) CD_{400} aqueous solution at different excitation wavelength (in 20 nm increment starting from 300 nm to 400 nm).

Table S1 Quantum yields of the CDs obtained at different temperature in different solvents

Temperature (°C)	NMP	Water	Ethanol	DMF
200	47	--------	--------	--------
300	41	15	31	7
400	25	--------	--------	--------

Table S2 Data on the reproducibility of the CD products, including the adsorption peak positions and maximum emission peak positions (λ_{ex} = 365 nm) for the CDs in aqueous solution and the corresponding quantum yields for the CDs in NMP solution.

Three Repetitive Experimental			
1st			
Sample	Absorption peak position [nm]	Maximum emission peak position [nm]	Quantum yields [%]
CD_{200}	223	380	46
CD_{300}	226	466	41
CD_{400}	224	427	23
2nd			
Sample	Absorption peak position [nm]	Maximum emission peak position [nm]	Quantum yields [%]
CD_{200}	222	383	47
CD_{300}	225	464	41
CD_{400}	226	424	25
3rd			
Sample	Absorption peak position [nm]	Maximum emission peak position [nm]	Quantum yields [%]
CD_{200}	225	376	47
CD_{300}	228	465	39
CD_{400}	225	428	24

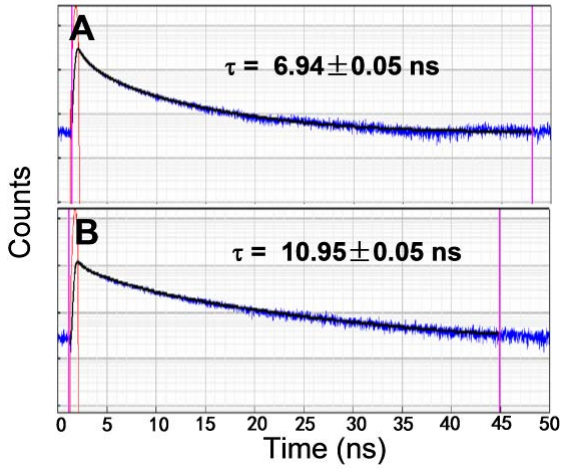

Figure S9. Time-resolved fluorescence decay curves of (A) CD_{200} and (B) CD_{400} powders measured at emission-peak maxima of 405 nm and 445 nm, respectively. The samples were excited at 380 nm.

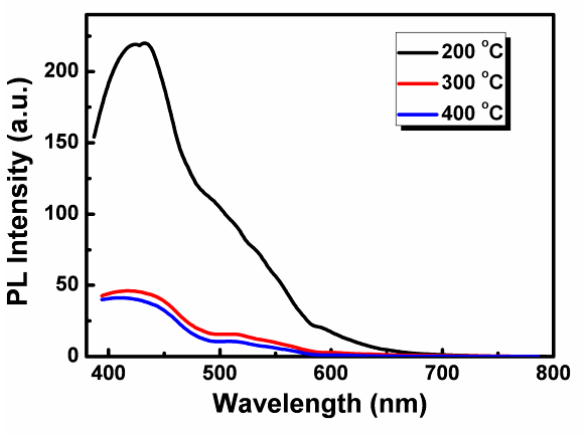

Figure S10. PL spectra of the samples obtained via pyrolysis of PS microspheres at different temperature.

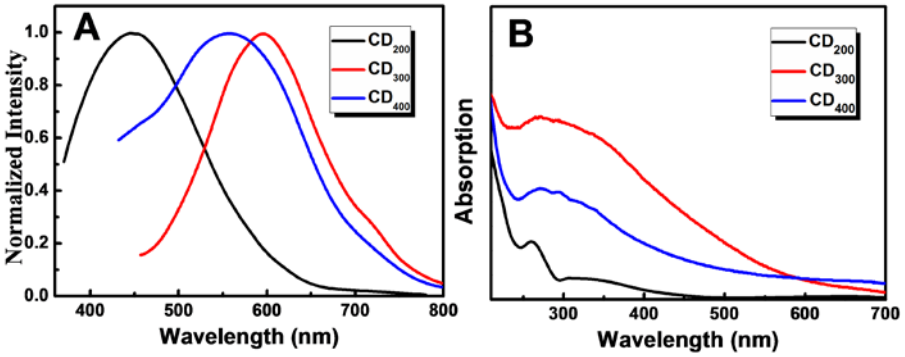

Figure S11. (A) PL spectra and (B) UV-vis spectra for condensed films of CDs.

3. Reference

(1) (a) A. G. Cano-Marquez, F. J. Rodriguez-Macias, J. Campos-Delgado, C. G. Espinosa-Gonzalez, F. Tristan-Lopez, D. Ramirez-Gonzalez, D. A. Cullen, D. J. Smith, M. Terrones, Y. I. Vega-Cantu, *Nano Lett.* 2009, **9**, 1527; (b) D. V. Kosynkin, A. L. Higginbotham, A. Sinitskii, J. R. Lomeda, A. Dimiev, B. K. Price, J. M. Tour, *Nature* 2009, **458**, 872; (c) L. Y. Jiao, L. Zhang, X. R. Wang, G. Diankov, H. J. Dai, *Nature* 2009, **458**, 877; (d) A. L. Elias, A. R. Botello-Mendez, D. Meneses-Rodriguez, V. J. Gonzalez, D. Ramirez-Gonzalez, L. Ci, E. Munoz-Sandoval, P. M. Ajayan, H. Terrones, M. Terrones, *Nano Lett.* 2010, **10**, 366; (e) J. L. Li, K. N. Kudin, M. J. McAllister, R. K. Prud'homme, I. A. Aksay, R. Car, *Phys. Rev. Lett.* 2006, **96**, 176101.

(2) H. Li, X. He, Z. Kang, H. Huang, Y. Liu, J. Liu, S. Lian, C. H. A. Tsang, X. Yang, S.-T. Lee, *Angew. Chem. Int. Ed.* 2010, **122**, 4532.